

Master Thesis project

A guided heuristic approach
to
the MEG inverse problem



Presented by:

Carlos Herrero Gómez

Supervised by:

Jose María Peña and Antonio LaTorre

Index

1. Introduction
 - Motivations
 - Basics of neurology
 - The neuron and the electric transport
 - Magnetostatics and SQUID
 - The direct and inverse problem
 - State of the art of solving methods for the inverse problem
 - Review of heuristic optimization methods
 - Examples of heuristic methods
 - Heuristic methods in MEG
2. Objectives
3. Results
 - A guided heuristic approach to the inverse problem
 - Restriction methods
 - Working framework and experimental procedure
 - Performance testing methods
 - Testing scenarios
 - Experimental results
4. Discussions
5. References

1. Introduction

Motivations

There is general agreement within the scientific community in considering Biology as the science with more potential to develop in the XXI century. This is due to several reasons, but probably the most important one is the state of development of the rest of experimental and technological sciences. In this context, there are a very rich variety of mathematical tools, physical techniques and computer resources that permit to do biological experiments that were unbelievable only a few years ago. Biology is nowadays taking advantage of all these newly developed technologies, which are been applied to life sciences opening new research fields and helping to give new insights in many biological problems. Consequently, biologists have improved a lot their knowledge in many key areas as human function and human diseases. However there is one human organ that is still barely understood compared with the rest: The human brain.

The understanding of the human brain is one of the main challenges of the XXI century. In this regard, it is considered a strategic research field for the European Union and the USA. Thus, there is a big interest in applying new experimental techniques for the study of brain function. Magnetoencephalography (MEG) is one of these novel techniques that are currently applied for mapping the brain activity¹. This technique has important advantages compared to the metabolic-based brain imagining techniques like Functional Magneto Resonance Imaging² (fMRI). The main advantage is that MEG has a higher time resolution than fMRI. Another benefit of MEG is that it is a patient friendly clinical technique. The measure is performed with a wireless set up and the patient is not exposed to any radiation.

Although MEG is widely applied in clinical studies, there are still open issues regarding data analysis. The present work deals with the solution of the inverse problem in MEG, which is the most controversial and uncertain part of the analysis process³. This question is addressed using several variations of a new solving algorithm based in a heuristic method. The performance of those methods is analyzed by applying them to several test cases with known solutions and comparing those solutions with the ones provided by our methods.

Basics of neurology

The brain is basically formed by two kinds of cells: Neurons and glial cells. The neurons are the ones in charge of the brain activity while glial cells only have a support role for the neurons. In particular they form part of the connective tissue. This is the reason why even though almost the 90 % of the human brain is formed by glial cells, the study of the brain function focuses on that other 10% and is commonly referred as neurology.

A neuron is the building block of brain activity. As it is shown in Fig (1) a neuron is composed by three main parts: the *body*, the *axon* and the *dendrites*. The body forms roughly 80% of a neuron volume and it contains the entire cell organules (the subcellular unities) .The body is surrounded by the dendrites which main role is to be the receptors of an *incoming signal* from another neuron, although sometimes they may act as emisors. Finally a neuron has a long, tail-shaped protuberance called the axon, which is usually in charge of sending the *outgoing signal*. Therefore, a neuron can be understood as a little input-output circuit, where usually the incoming signal is received in the dendrites, it is processed in the body and it is emitted by the axon. The information is transmitted via electric signals. This fact is exploited by MEG to get information about the brain activity. The mechanism of electric transport in the human brain will be developed with more detail in the next subsection:

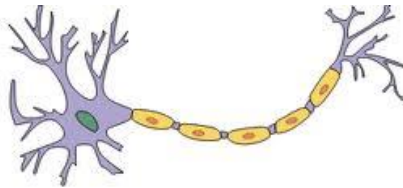


Fig 1. Sketch of a neuron

The neuron and the electric transport

A neuron, like every cell, has a phospholipid membrane with features similar to a liquid crystal and a thickness about 10 nm. The role of this membrane is to isolate the cell from the extracellular fluid, but allowing at the same time a selective exchange between inside and outside the cell.

For a proper physiological work (homeostasis), the extracellular and intracellular compartments must have different ionic concentrations. In order to keep that different concentration, the cells have certain protein molecules scattered in the membrane , which are often referred as the *fluid mosaic*, due to it liquid crystal properties. These proteins bomb some ions against the concentration gradient. Thus they are called *ionic bombs*, such as the Na-K bomb⁴.

The resting electric potential condition is achieved when the diffusive and ohmic currents in addition to the bombing currents are compensated for each ion specimen. In last term, the equilibrium is governed by the specific permeability of the membrane to the different kind of ions.

A synapse is a structure that permits a neuron to communicate or pass a signal to another cell making use of the properties of the aforementioned proteins. There are basically two kinds of synapses:

A *chemical synapse* is based in the release of ions. It is triggered by the opening of voltage gated calcium channels. The opening of those channels lead to the release of biochemical molecules called *neurotransmitters*. Neurotransmitters bind to receptors located in the postsynaptic cell, causing a change in the relative permeability to certain ions. This change of the relative permeability catalyzes the movement of ions out or in the cell, leading to a voltage difference and, as a consequence, to an electric current.

The second type is called, an *electric synapse*, where both neurons are joined by special channels, the so-called gap-junctions, which allow transmitting directly an electric current. These types of synapses are much faster in transmitting the information than the chemical ones.

For the purpose of the current work, the crucial fact is to realize that every synapse or neuron connection leads to a current transport that may be modeled as a current dipole. A current dipole, as will be shown in the next section, is also a magnetic field source. If this magnetic field is measured, it is possible to obtain information about the position of the dipoles responsible of that field. That would be equivalent to know the position of the synapses. This is the ultimate objective of the magnetoencephalography, and of course, it is a task full of technical and conceptual challenges.

Magnetostatics and SQUID

The Electromagnetism is ruled by the Maxwell equations, that are usually given as example of the beauty of physical rules due to their completeness and symmetry. The Maxwell equations are given in *Eqs (1)*:

$$\begin{aligned}\nabla E &= \frac{\rho}{\epsilon_0} \\ \nabla \times E &= -\frac{\partial B}{\partial t} \\ \nabla B &= 0 \\ \nabla \times B &= \mu_0 \left(J + \epsilon_0 \frac{\partial E}{\partial t} \right)\end{aligned} \quad Eqs (1)$$

In these equations, \mathbf{E} and \mathbf{B} stand for the electric and magnetic fields respectively, ρ and J are the electric charge and electric current densities and finally the constants ϵ_0 and μ_0 are the permittivity and susceptibility of the vacuum.

The magnetostatic approach consists in neglecting the time derivatives terms in *Eqs (1)*. This can be justified for physiological reasons as is explained by A.Hoyos et al.⁵

In a MEG analysis, the sources are the current density J that will be usually modeled as current dipoles located at some fixed positions r_Q :

$$J^P = Q\delta(r - r_Q) \quad Eq (2)$$

On the other hand, the experimental data consists in measurements of the magnetic field \mathbf{B} created by those sources at certain points outside the brain.

One of the main technological handicaps of the MEG is that the brain function generates a very low intense magnetic field. Furthermore, we are continuously surrounded by much higher intensity magnetic field that completely mask the one coming from the neural activity. Some examples of those fields are the *earth magnetic field* that arises from the rotation of the ionosphere, the charged layer of the atmosphere, and the magnetic field generated by all kind of electronic devices.

Accordingly, it is crucial to both isolate the chamber where the MEG experiment is carried out and also to use the most precise equipment to measure that magnetic field.

Therefore, a MEG experiment is always performed in isolated chambers, and the measurement is done using a *SQUID* (Superconductor QUantum Interference Device). This device consists of a superconductor ring interrupted by one or two Josephson unions.⁶ This particular arrangement leads to the most precise magnetic field sensor that is nowadays available.

The direct and inverse problem

One of the key concepts to fully understand the implications of a source reconstruction based on a MEG measurement is the difference between a direct and an inverse problem.⁷

In this context, the *direct problem* deals with the calculation the magnetic field at any point created by a certain *known* distribution of current. This problem has an unique solution, and it is straightforward to solve using *Eqs (1)* if all the parameters of the media are known (i.e. the conductivity in the different brain tissues). In the MEG jargon the solution to the direct problem is often called the Lead field \mathcal{L} . The lead field fulfills the following equation:

$$\vec{Y} = \mathcal{L} \vec{X} \quad Eq (3)$$

Where \vec{Y} represents the sensor measurements of the magnetic field and \vec{X} stands for the current distribution.

The Lead field can also be understood as a transformation between the source space to the space of sensors. The *inverse problem* addresses the question of finding the inverse transformation of the Lead field (i.e. from the sensor space to the source space). This is actually the goal of the MEG, to map the brain activity, starting from the sensor data. Both the direct and inverse problems are schematically shown in Fig (2).

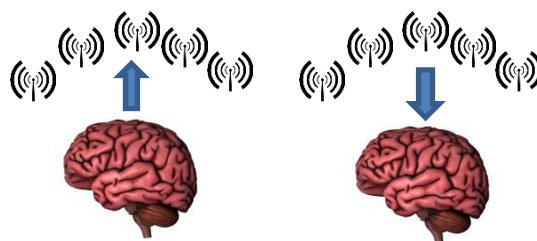


Fig 2. Sketch of the direct (left) and inverse (right) problem

The *inverse problem* does not have a unique solution. This means there are an infinite set of possible solutions to that problem. This absence of uniqueness is the biggest conceptual

challenge of the MEG analysis. In practice some constraints must be added in order to narrow down that number of solutions and select one.

The different MEG solving methods differ in the constraints that are taken into account. Due to the complexity of the problem, and to the fact that it is a new research area, there is still not a clear agreement within the research community concerning which is the best analytical method.

State of the art of solving methods for the MEG inverse problem

There are a huge variety of solving methods for the MEG inverse problem. However, there are two different types that are the most commonly used and carefully studied. Those methods are the so-called *least squares or minimum-norm methods* and the *beamformers*.

The minimum norm method

This strategy is based on searching for a particular arrangement of sources X that minimizes the following cost function:

$$F(Y, X) = |Y - \mathcal{L}X| \quad Eq (4)$$

Where the matrix Y represents the experimental data in the space of sensors and \mathcal{L} is the leadfield, or solution of the direct problem. This function may be applied to a certain time measurement or to a time averaged data. Those approaches are called the *fixed* or *oscillating dipole* approximations.

One problem of this method is that the number of sources must be decided *a priori*, although a good approximation could be estimated from the rank of the experimental data. However the most challenging drawback of this method is the so called *overfitting*. *Overfitting* means that for high enough number of sources there exists infinite solutions of source arrangement that minimizes the cost function $F(Y, X)$. Usually in optimization problems, the main goal of the solving methods is to avoid local minima and to find the global one. In this case, the actual difficulty is not to find the global minima of the cost function. The real problem is that the cost function $F(Y, X)$ *does not have* a global minimum but infinite local minima. This issue is overcome by adding constraints to the fitness function, both mathematical of physiological, so the number of possible solutions is decreased.

Beamforming methods

This approach uses a space filter to choose only some data points coming from a certain region. Ideally this spatial filter would fulfill the following equation:

$$W(r_q) \mathcal{L}(r) = \begin{cases} 1 & \text{if } |r - r_q| < \delta \\ 0 & \text{if } |r - r_q| > \delta \end{cases} \quad Eq(5)$$

The problem is that it is impossible to calculate a set of filters $W(r_q)$ that fulfill *Eq (5)* for every point $r_q \in r$ due to the limited number of degrees of freedom. Then the space filters are approximated using some optimization approach as is the example of the LCMV (Linearly Constrained Minimum Variance) or DICS (Dynamic Imaging of Coherent Sources).

Review of heuristic optimization methods

Most of the solving methods that were previously described implied an optimization at some step of the process. This is especially true in the case of the minimum norm methods, that are basically a minimization of the cost function, given by Eq (4).

Since our proposal will be based on a heuristic method, this chapter will be a brief summary of some of the most important heuristic techniques. Firstly, it will be introduced the motivation of a heuristic approach. Secondly it will be explained the concept of the heuristic approach as well as some of the most popular heuristic strategies.

In order to choose a method to solve an optimization, the key factor to be taken into account is the epistasis of the problem. The epistasis represents how the cost function depends on the relationships between the variables of the problem. Simplifying, when the different variables of the cost function do not depend on the others (or they depend only slightly) it is said to be a low epistasis problem. On the other hand, if a problem has a high degree of epistasis, a slight change in one variable will lead to huge changes in all the rest and on the fitness function.

Therefore, an optimization problem with very low epistasis can be successfully solved using direct analytical methods (a gradient based method). On the other hand, in the extreme case of a huge epistasis problem no searching method would give any better performance than a completely random inspection of the whole space of solutions. The heuristic methods are the best approach to face problems with intermediate epistasis, as it shown in Fig (3). This is the case of the MEG inverse problem.

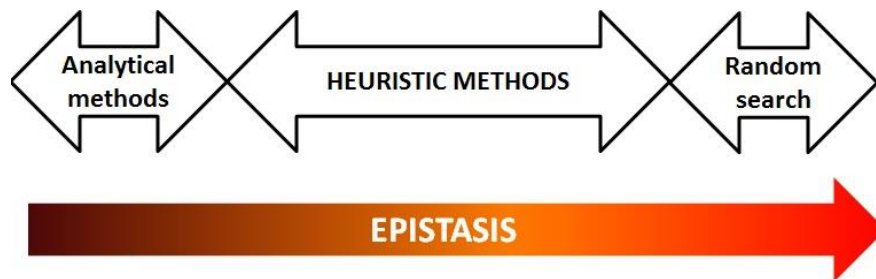


Fig 3. The best optimization strategies for different epistasis-level problems

A heuristic approach consists of a guided or experience based method to solve an optimization problem without exploring the whole space of solutions. The heuristic search combines a degree of randomness and guided search, giving rise to important speed up performance in problems when the exhaustive search is impractical or impossible (medium-high epistasis). There will be introduced three of the most popular heuristic methods:

Examples of heuristic methods

- **Genetic Algorithms (GAs)**

A genetic algorithm starts with the initialization of a certain number of candidate solutions. In the genetic algorithm jargon, each possible solution is called *individual*, each of the different variables within a solution is called *gene*, and the total number of individuals is often referred as *population*. That population is ranked based on the cost function to be optimized and the individuals are matched based on that ranking. Then a new population is produced by selectively crossing the genes of the father and mother and adding a possibility of mutation to those genes. That step is called the *reproduction*. After the reproduction, the new generation consists of a combination of the offspring individuals and the old generation ones. The amount of individuals that are kept from the last generation is called the *elitism* of the algorithm.⁸

This process of the evaluation, selection and reproduction takes places iteratively until an stop condition is reached, typically when a convergence or time criteria is met. Once the termination condition is achieved the solution is picked as the best ranked one of the last generation. The flowchart of a genetic algorithm is shown in Fig (4).

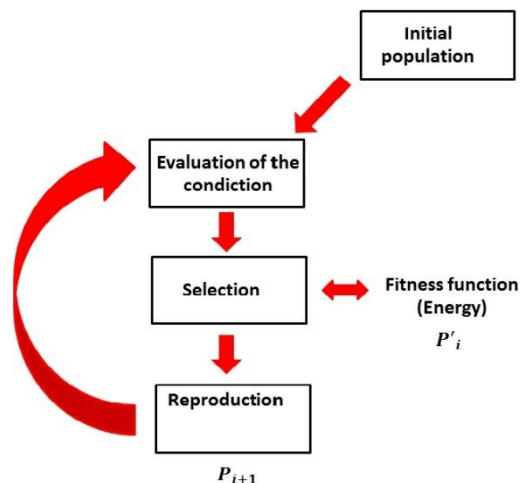


Fig 4. Flowchart of a genetic algorithm

- **Simulated annealing (SA)**

This heuristic method takes its name from a well-known technique in metallurgy. The annealing and cooling technique is used in material science to change the microstructure of a solid by providing thermal energy to the atoms. This way they can move and re-arrange themselves in a new energetically better configuration. A material in equilibrium has a microstructure such that its free energy is placed in a local minimum. If some energy is supplied to the solid it eventually will be able to *jump* from this minimum to a higher energy state which was previously inaccessible. If the material is cooled afterwards it will evolve to an energy minimum which can be different from the initial state, leading to a new equilibrium microstructure. This process is schematically shown in Figure (5).

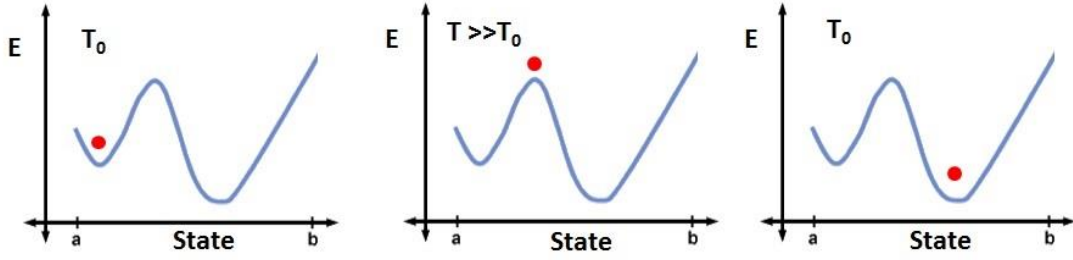


Fig 5. Scheme of the effect of annealing in the microstructure of a crystal.

This same working principle is used by the simulated annealing algorithm⁹ (SA). In a SA algorithm the system is initialized in a certain state and with a certain value of a parameter called *temperature*. The temperature value will decrease as the iteration number increases.

Then, each iteration, some neighbor states are calculated, within a distance from the current state usually proportional to the temperature. Afterwards the system probabilistically decides to move to a neighbor state or to stay in the current state. A common approach is to always accept a new solution if it has a better fitness than the old one. In the case that it has worse fitness, it is accepted with a probability following a Maxwell distribution given by Eq (6):

$$P = e^{-\frac{E}{k_B T}} \quad \text{Eq (6)}$$

The consequence of the decreasing value of the temperature with the number of iteration is that in the beginning, the system is allowed to undertake big changes, so it easily explores the whole solution space. On the other hand, when the algorithm is finishing (last iterations) the temperature is low, so the system will only be allowed to move to a local minimum which hopefully will be the global one if the exploration in the early stages was good enough.

- **Differential evolution algorithm (DE)**

This is one of the simplest heuristic methods but it is still one of the most popular techniques within the numerical analysts because of its robustness. It is very similar to a genetic algorithm but in this case the reproduction of the different individuals is carried out by a linear combination of other individuals.¹⁰

The most popular reproduction algorithm is to generate the offspring gene by gene. It is done by allowing a certain probability to just copy the gene of the father to the offspring, and another probability to generate this gene as a linear combination of the genes of other individuals, following Eq (7):

$$x_j^{i+1} = x_j^i + F(a_j^i - b_j^i) \quad \text{Eq. (7)}$$

Where subindex j stands for the number of gene within the solution X , i is the generation subindex and a and b represent different individuals. After the generation of the new individual, both the precursor and the offspring are ranked based on the cost function and the best ranked one will survive to the next generation.

The Heuristic methods in MEG

The MEG inverse problem can be posed as an optimization problem. The goal of such optimization problem is to find a current distribution that minimizes the following fitness function:

$$F(Y, X_{sim}) = |Y - \mathcal{L}X_{sim}| \quad Eq. (8)$$

Minimizing Eq (8) is equivalent to minimize the differences between the experimental sensor data and the sensor measurement that would produce a candidate source distribution X_{sim} .

As was previously stated, there are an infinite number of solutions X_{sim} that would minimize $F(Y, X_{sim})$. In order to narrow down that number, constraints are added to the solving method.

2. Objectives

The objectives of the current work are described in the following paragraphs:

- Introduction of the Magnetoencephalography and its working principles
 - Electromagnetism
 - SQUID
 - Data analysis
 - Optimization techniques
- Identification of the main current challenges in MEG analysis
- Proposal of a solving method for the MEG inverse problem
 - Motivations of the method
 - Description of the technique
 - Test of the method performance
 - Quantitative analysis
 - Qualitative analysis
- Results and discussion

3. Results

A guided heuristic approach to the inverse problem

The main goal of the present work is to present a new solving method for the MEG inverse problem and to analyze its performance by testing it in different scenarios.

First of all, it will be introduced the method, a guided heuristic algorithm, and its motivations. After that, the key part of the algorithm will be detailed step by step. Finally there will be described the working framework and the experimental procedure for testing the results.

The chosen procedure basically consists of a constrained minimum norm or least square algorithm solved using a Differential Evolution algorithm. The search space of this DE algorithm is limited to few values instead of being able to explore the whole solution space. The motivation to do this is to avoid *overfitting*, that was previously described. The goal of this particular method is to discard the less likely of those possible arrangements and focus the algorithm search on the subspace of the most probable solutions. This constriction is achieved by a selective initialization of the DE algorithm, so all the further search will be constrained. In the present work there are introduced four different types of restriction methods.

In the following section it will be described the key part of the algorithm, which is the restriction method.

Restriction methods

As was stated in the former section, this source estimation method consists of a minimum-norm constrained to a certain subspace on the solution space. This restriction is critical, because although it may help to avoid *overfitting*, if it is not carefully done, it may as well exclude the correct solution from the search space.

Actually the working principle of this method is to search for the most probable of all the possible source configurations that would lead to a given sensor measurement. To do so, some assumptions were made:

- i) *Localized sources*: The algorithm will focus on the search of *localized sources*. Any field distribution may be created by a noisy activation of all the source points, but instead of looking for that kind of configurations, the algorithm will try to look for a source distribution that replicates the experimental measurement with the minimum number of involved sources.
- ii) *The easiest solution*: Among the solutions involving few sources (the first assumption) the algorithm's aim will be to select the most probable one. This is achieved by selecting the source points with important gain in all the highly activated sensors at the same time.
- iii) *The minimum energy solution*. The last assumption is that between different configurations, the correct one will be the one with the minimum magnetostatic energy. The magnetostatic energy of a set of dipoles is given by Eq (9):

$$E_{mag} = \sum_i^n |\vec{m}_i|^2 \quad Eq (9)$$

The minimum energy assumption is taken into account adding the term given by Eq (9) to the cost function to be minimized by the method. Thus, the final cost function is given by Eq (10).

$$F(Y, X_{sim}) = |Y - \mathcal{L}X_{sim}| + \alpha |X_{sim}|^2 \quad Eq (10)$$

The first two assumptions are incorporated in the initialization process of the DE algorithm doing the following procedure:

Firstly, the experimental data is analyzed to select the most activated sensors. In order to do so, the sensors whose intensity signal fulfills the condition given by Eq (11) are selected:

$$|I_i| \geq \frac{|I_{max}|}{2} \quad Eq . (11)$$

Where i represents the channel (or sensor) index, and I_{max} is the intensity of the sensor with the highest signal. These values will be referred as *principal sensors*, and will be the ones that will be taken into account to choose the search subspace. The indexes of these principal sensors are stored in the vector \vec{n} . Once the principal sensors are selected, the algorithm explores which source points have more gain in that principal sensors. The gain of a source point i over a sensor n is defined by Eq (12):

$$G_n^i = |\mathcal{L}_{n,1}^i| + |\mathcal{L}_{n,2}^i| + |\mathcal{L}_{n,3}^i| \quad Eq. (12)$$

Where $\mathcal{L}_{j,k}^i$ stands for the j -row and k -column term of the lead field of the source location i . Thus, G_n^i is the sum of the gains of the three components (x, y, z) of a dipole located in the position i on the sensor channel n . When the information of the gain is available, the algorithm computes the so called matrix of influences \hat{I} . That matrix is a $n \times k$ matrix being n the length of \vec{n} , and k an arbitrary number, set to 10. Each row i contains the list of points with biggest gain with respect to that sensor in decreasing order of gain. Afterwards the algorithm counts the number of times that each of the points of the matrix of influences appears in the matrix. Finally, those points are sorted in decreasing order of time of repetitions.

In this step, the algorithm allows four selecting methods for the search subspace. The *first method* is to select the top 10 most repeated points of matrix \hat{I} as seed points of the search space. Afterwards, a number N of nearest neighbors is added to each of the already selected

seed points. The neighbors are selected as the closest grid points to each of the seeds in the source space using the classic Euclidian distance. Finally, the search subspace is set as those seed points together with their respective neighborhoods.

The *second method* allows all the points of matrix \hat{I} to be selected for the search space but with a probability proportional to the number of repetitions in that matrix. This way the most repeated points (the ones with highest gain to several sensors) are given more probability to be selected for the subspace, but giving a little chance to other source points that were automatically discarded in the first method. As in the previous case, a neighborhood is added to each of the selected points.

The *third and fourth methods* are modifications of the first two ones. These methods allow the system to explore the *whole space of solutions*, but the points that do not belong to the subspaces calculated by the methods 1 and 2 are initialized with a very low intensity.

The ratio of the initial intensity of the subspace points to the rest of the points was set to 20. Consequently, these methods will be called *noisy methods* while the first and second methods will be referred as *concentrated methods*.

Working framework and experimental procedure

This project was developed using the Fieldtrip Matlab toolbox as general framework. Fieldtrip is a collaborative toolbox for EEG/MEG analysis developed by different international research groups and is nowadays one of the most popular softwares for MEG analysis¹¹.

Fieldtrip includes codes for different methods of simulation of the direct problem, inverse problem and a vast amount of data, both MEG and anatomical. The anatomical information is provided by a Magnetic Resonance Image (MRI) that is used as spatial reference for the MEG. The work was developed using as starting point all the available resources from Fieldtrip, but replacing the Fieldtrip source location algorithms by the method to be tested.

All the simulations were run using the subject called “Subject.1” as testing patient. The direct problem solution (the Lead field \mathcal{L}) was also calculated using Fieldtrip software for the particular case of a CTF MEG equipment with 149 channels. To solve the direct problem Fieldtrip divides the brain volume in a grid with a total of 3042 points, divided in 1448 inner points (points allowed to have an electric dipole) and 1558 outer points. For each of the inner points there are three variables corresponding with the three spatial components (x,y,z) of the intensity of the electric dipole, leading to 1484 x 3 unknowns for the inverse problem. Since the brain volume is discretized so is the Lead field, which is represented by 1484 (3x149) matrixes. Therefore, the recorded signal in the sensors can be calculated making use of Eq (13):

$$Y = \sum_i^{1484} \mathcal{L}_i X_i \quad Eq(13)$$

Where \mathbf{Y} is a (149x1) vector that represents the magnetic field recorded in each of the sensors (channels), \mathcal{L}_i are the 1484 (149 x 3) matrixes that represent the gain spectrum of a dipole

located in the position i , and finally \mathbf{X}_i are (3x1) matrixes with the intensity of the three components of an electric dipole located at the grid point i . The source distribution \mathbf{X} can be displayed together with the anatomical data by interpolating the virtual grid of 3042 points with the MRI.

The objective of the inverse problem is to be able to reconstruct \mathbf{X} using as input the sensor measurements \mathbf{Y} and the solution of the direct problem, the lead field \mathcal{L} . This work focuses on the solution of the inverse problem for a single time instant, statistics are not applicable.

Performance testing methods

In order to test the performance of the solving methods, they were applied to a problem with a known solution. The four methods were tested in twelve different scenarios. For each of those scenarios the same procedure was followed:

1. A current distribution was numerically generated for the brain volume \mathbf{X}_{test} . Each of the twelve different scenarios were generated with different distributions.
2. Using Eq (8) the sensor signal created by those distribution was calculated and stored in the variable \mathbf{Y}_{exp} . This data and the Lead field \mathcal{L} will be given as input for the solving methods
3. The inverse problem defined by \mathbf{Y}_{exp} and \mathcal{L} is solved using the four different methods. The solution for each method is a current distribution \mathbf{X}_{sim}
4. the performance of the methods is analyzed from a quantitative and qualitative point of view.

- **Quantitative method**

The performance of each method is numerically ranked by comparing the solution \mathbf{X}_{sim} with the real sources \mathbf{X}_{test} . In order to have a quantitative measurement of the quality of the method, the following quality metric Q is computed:

$$Q = \sum_i^N \sum_j^{x,y,z} |\mathbf{X}_{test}^{i,j} - \mathbf{X}_{sim}^{i,j}| \quad Eq(14)$$

Where the sum is extended to all the source points and to all the three spatial components x, y, z . Low values of Q correspond to high quality solutions whereas high values of Q are related with low quality solutions. The quality factor Q will be analyzed for all the variations of the solving method, and for the twelve scenarios. This way, it will be possible to draw some conclusions about the performance of each method for different source arrangements.

- **Qualitative method**

The solution of the inverse problem \mathbf{X}_{sim} is interpolated with the MRI anatomical data and the same is done for the test source distribution \mathbf{X}_{sim} . As a result, the

quality of the method can be estimated by visual inspection of both anatomical images.

Testing scenarios:

The four variations of the method were tested in twelve different scenarios in order to check their validity for diverse source arrangements. A description of each of those scenarios is given in Table 1, while the anatomical representation of each of them is displayed in Fig (6).

Scenario 1	One single dipole located on a corner in top of the brain (point 1448)
Scenario 2	One single dipole located centered on the top of the brain (point 1464)
Scenario 3	One single dipole located in the middle of the brain volume (point 700)
Scenario 4	One single dipole located on the bottom of the brain volume (point 1)
Scenario 5	Two independent close-located dipoles both located on the top of the brain (positions 1484 and 1464)
Scenario 6	Two independent far away located dipoles one located on the top and one on the bottom of the brain.(positions 1484 and 1)
Scenario 7	Scenario 1 plus an isotropic random excitation of the rest of dipoles (white noise)
Scenario 8	Scenario 2 plus an isotropic random excitation of the rest of dipoles (white noise)
Scenario 9	Scenario 3 plus an isotropic random excitation of the rest of dipoles (white noise)
Scenario 10	Scenario 4 plus an isotropic random excitation of the rest of dipoles (white noise)
Scenario 11	Scenario 5 plus an isotropic random excitation of the rest of dipoles (white noise)
Scenario 12	Scenario 6 plus an isotropic random excitation of the rest of dipoles (white noise)

Table 1. Description of each of the experimental scenarios

Anatomical representation of the different scenarios

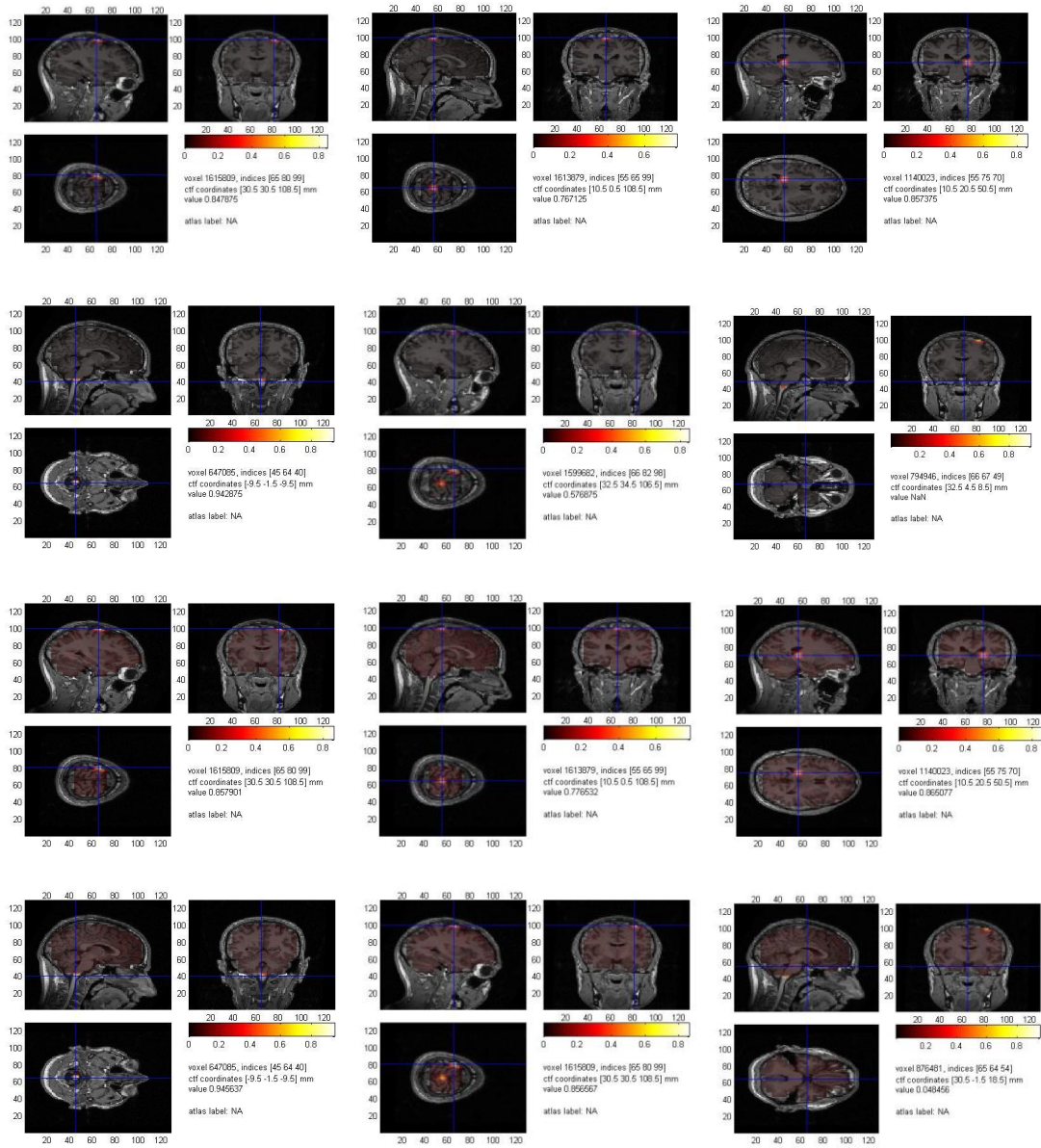


Fig 6. Interpolation of the test source distribution with the MRI anatomical data

Experimental results

In this section there will be presented the source reconstruction performed by the four variations of the method on each of the twelve different scenarios. In addition, it will be done a comparison of the performance of each method by comparing their quality factor Q . Finally the results will be discussed.

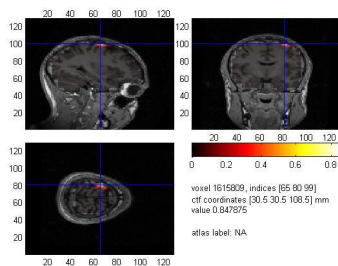
A brief summary of the differences between the methods, is presented below:

- Method I: *Concentrated* method, top 10 most repeated points selected as seeds.
- Method II: *Concentrated* method, seed points selected with some probability.
- Method III: *Noisy* version of method 1.
- Method IV: *Noisy* version of method 2.

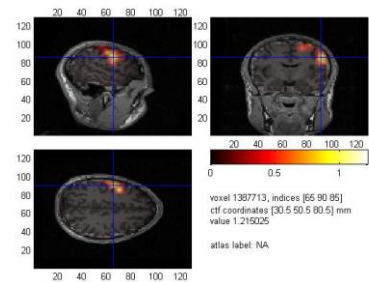
METHOD I

Scenario 1

Test sources

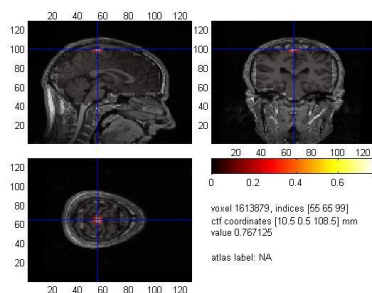


Simulation results

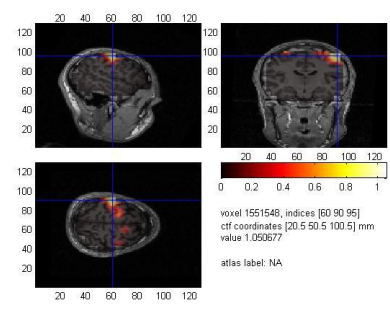


Scenario 2

Test sources

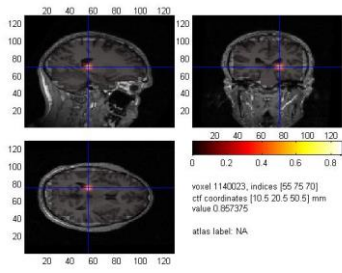


Simulation results

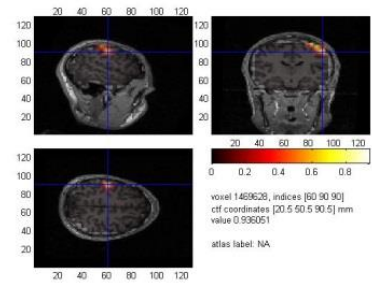


Scenario 3

Test sources

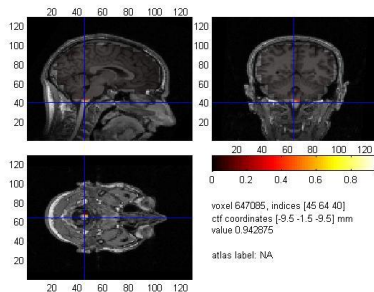


Simulation results

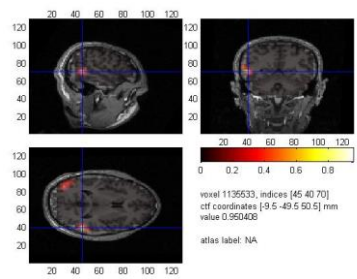


Scenario 4

Test sources

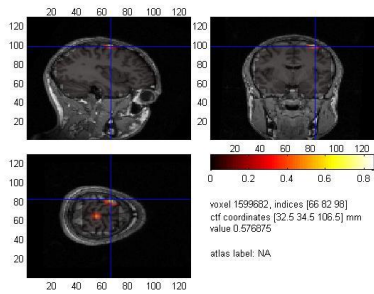


Simulation results

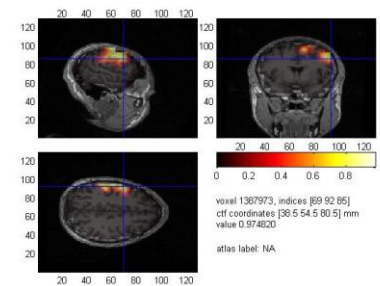


Scenario 5

Test sources

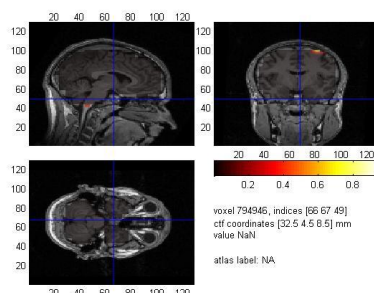


Simulation results

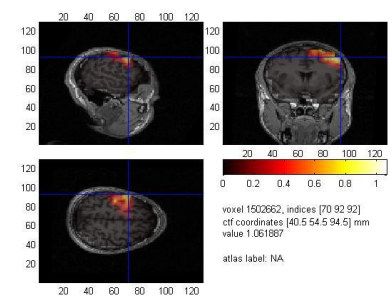


Scenario 6

Test sources

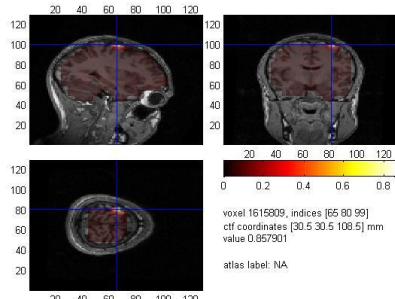


Simulation results

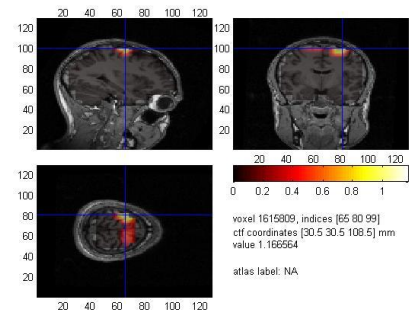


Scenario 7

Test sources

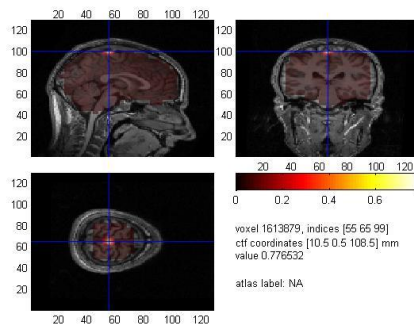


Simulation results

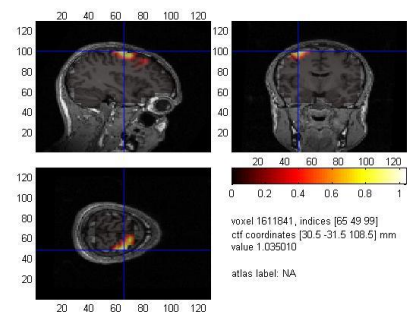


Scenario 8

Test sources

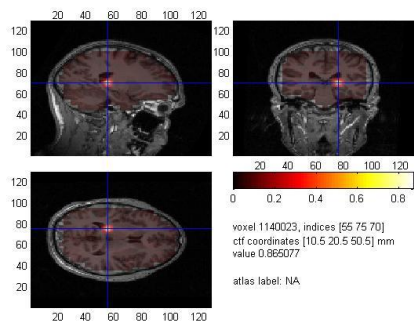


Simulation results

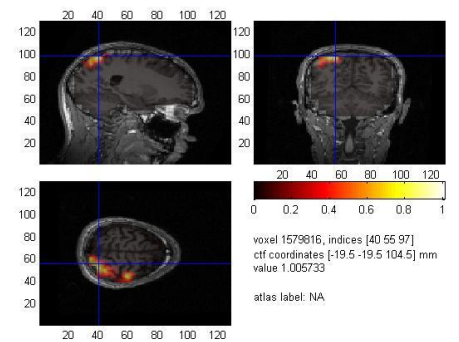


Scenario 9

Test sources

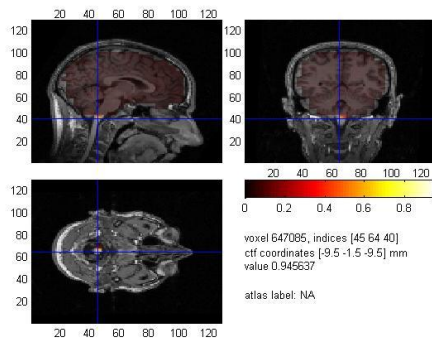


Simulation results

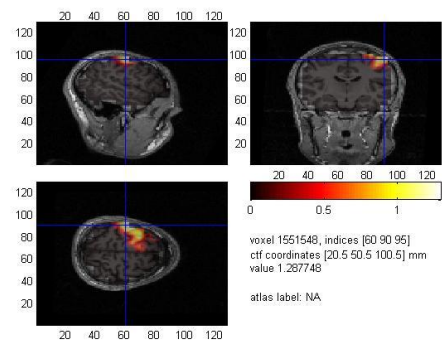


Scenario 10

Test sources

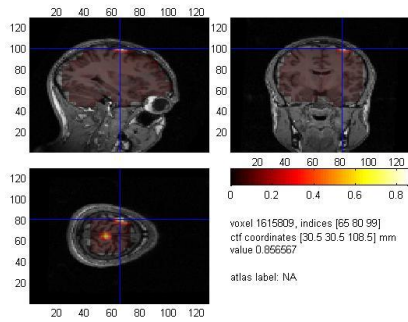


Simulation results

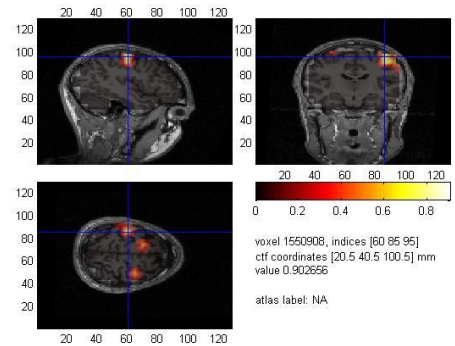


Scenario 11

Test sources

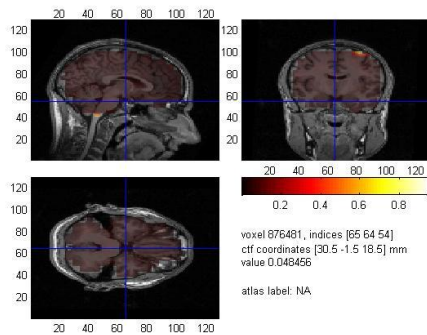


Simulation results

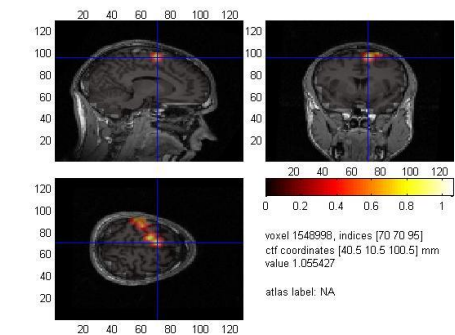


Scenario 12

Test sources



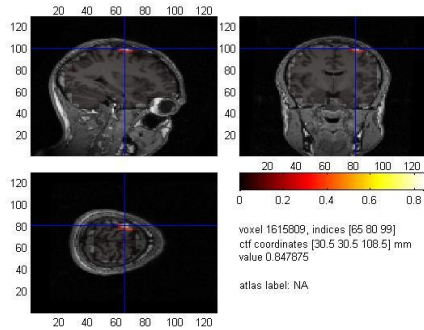
Simulation results



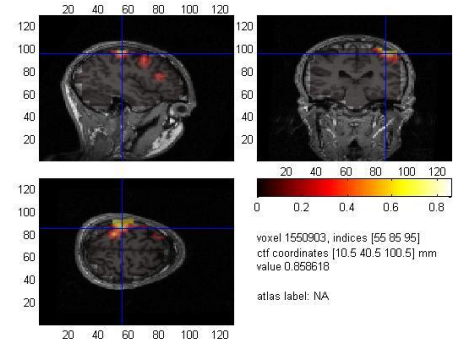
METHOD II

Scenario 1

Test sources

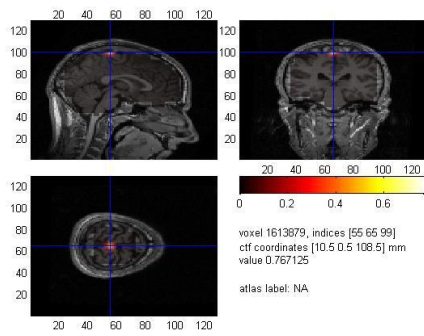


Simulation results

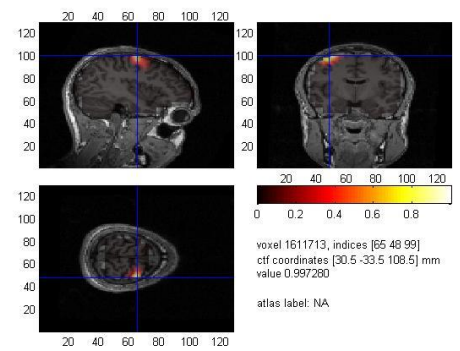


Scenario 2

Test sources

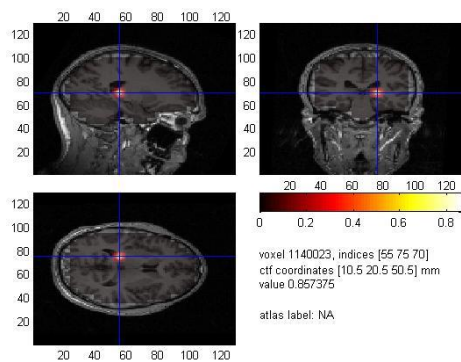


Simulation results

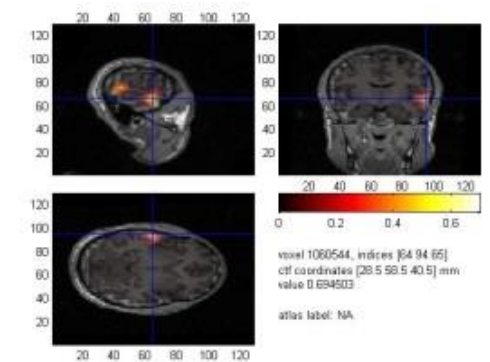


Scenario 3

Test sources

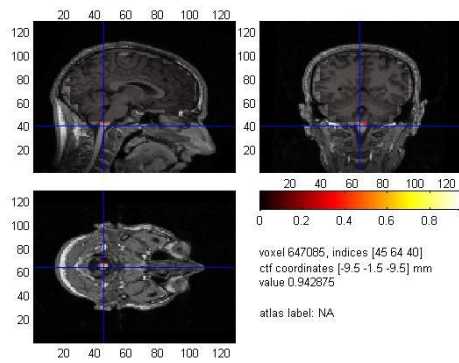


Simulation results

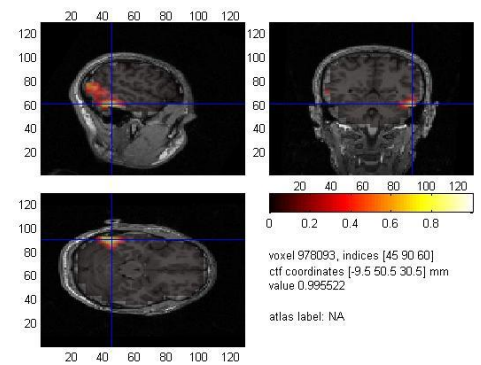


Scenario 4

Test sources

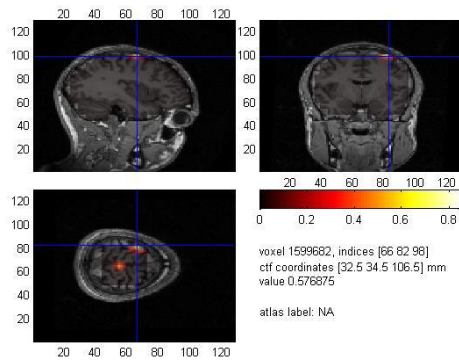


Simulation results

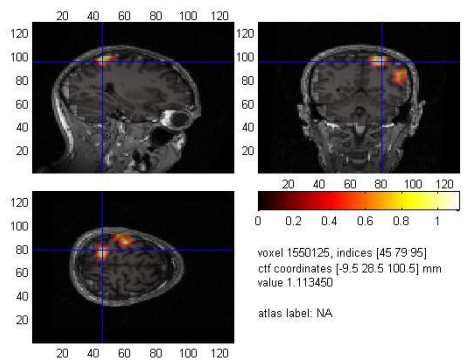


Scenario 5

Test sources

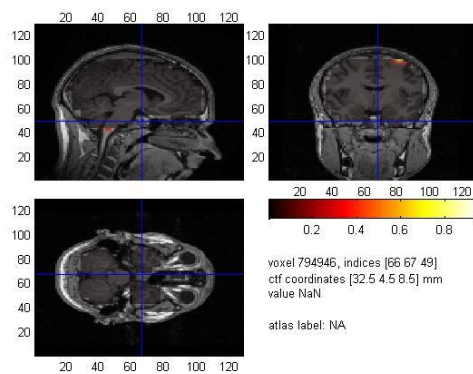


Simulation results

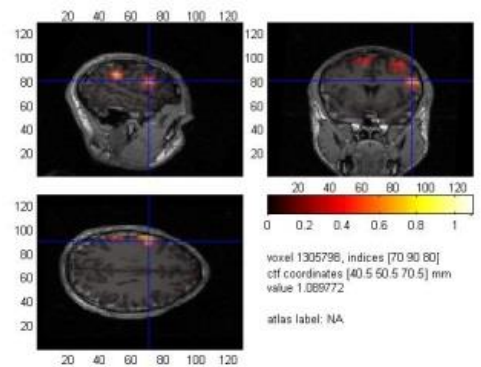


Scenario 6

Test sources

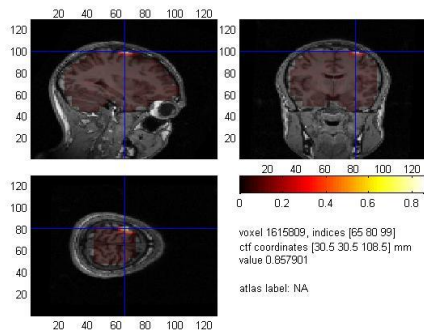


Simulation results

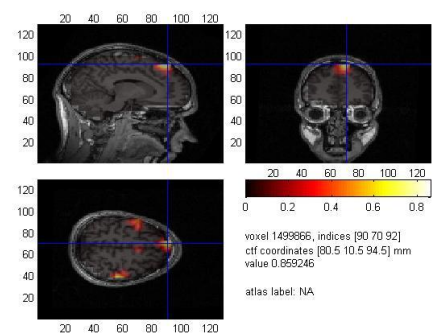


Scenario 7

Test sources

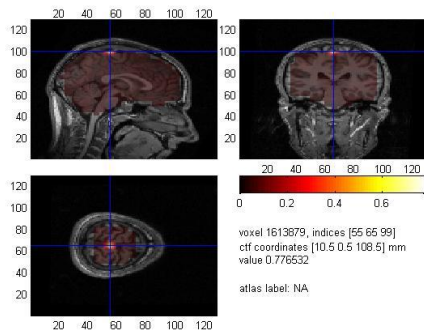


Simulation results

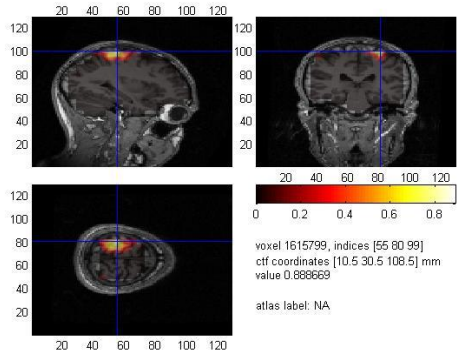


Scenario 8

Test sources

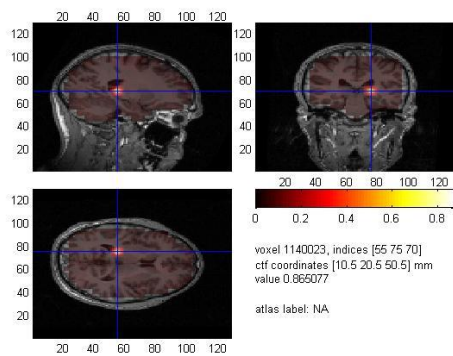


Simulation results

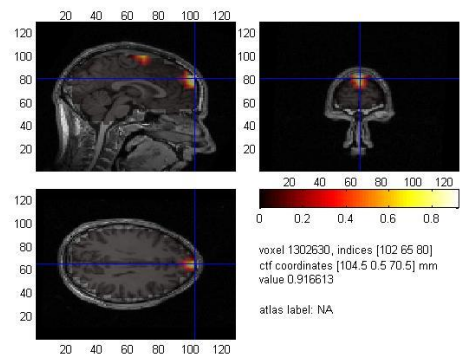


Scenario 9

Test sources

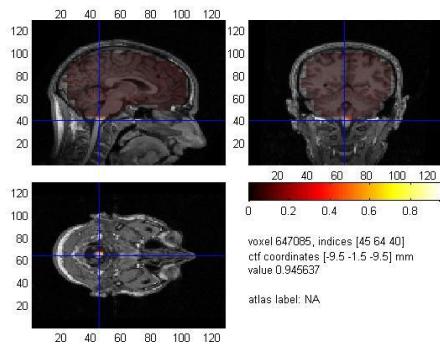


Simulation results

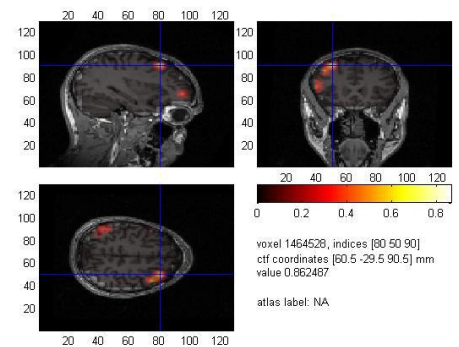


Scenario 10

Test sources

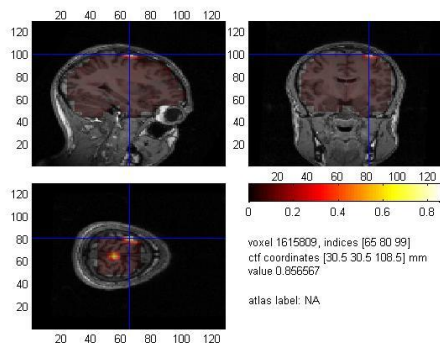


Simulation results

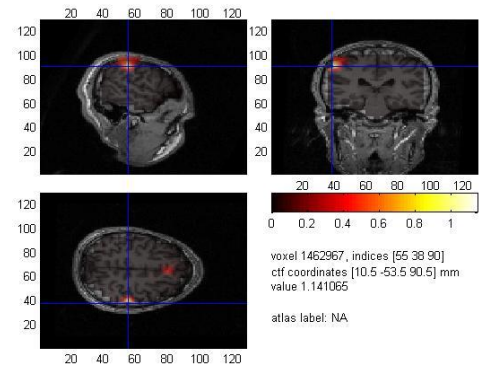


Scenario 11

Test sources

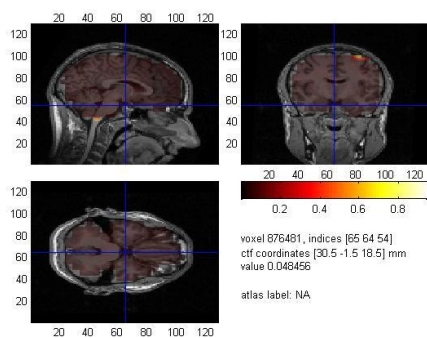


Simulation results

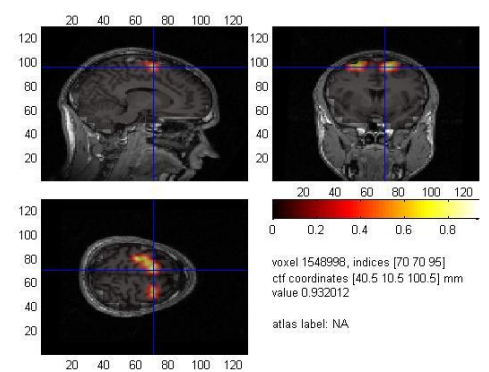


Scenario 12

Test sources



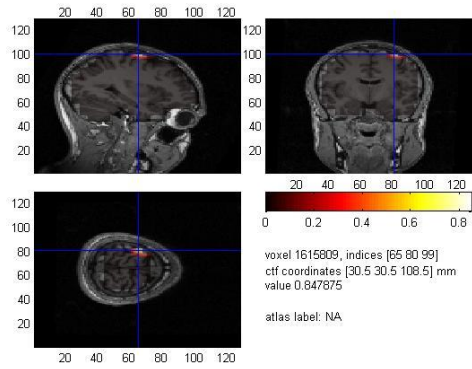
Simulation results



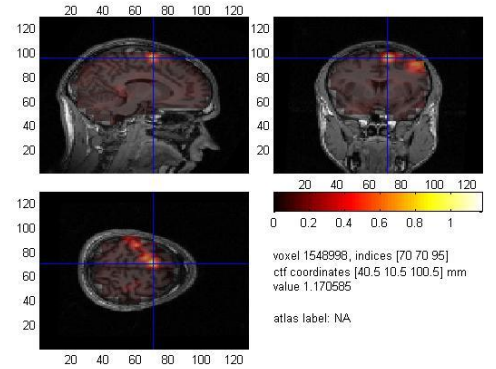
METHOD III

Scenario 1

Test sources

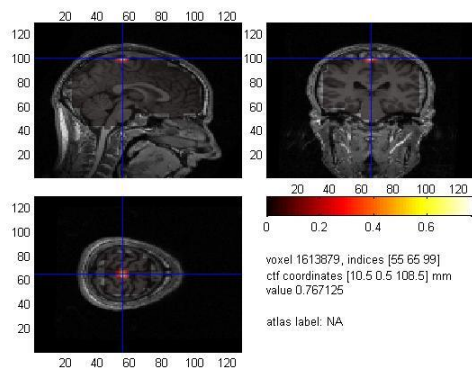


Simulation results

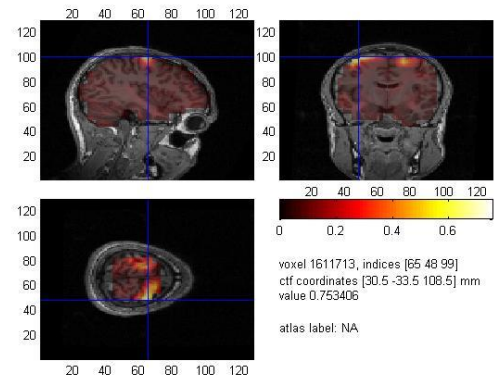


Scenario 2

Test sources

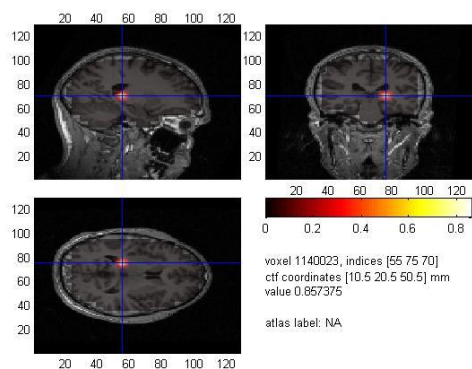


Simulation results

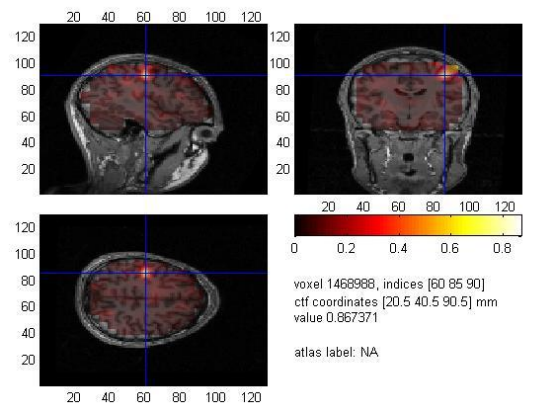


Scenario 3

Test sources

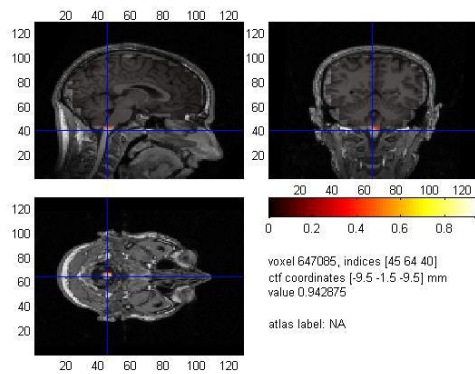


Simulation results

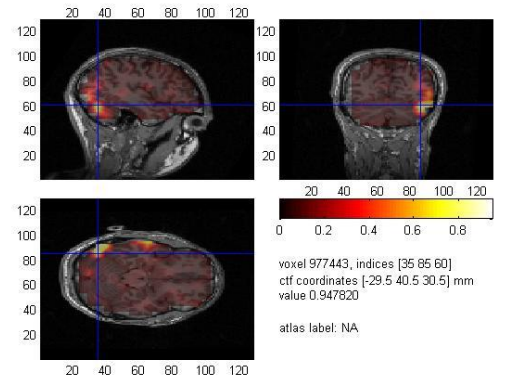


Scenario 4

Test sources

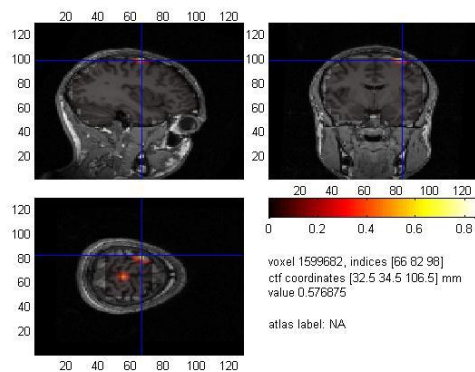


Simulation results

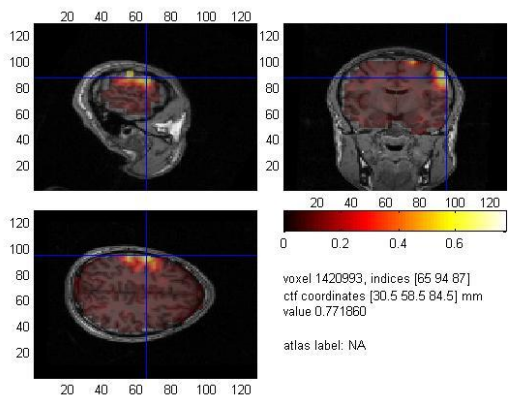


Scenario 5

Test sources

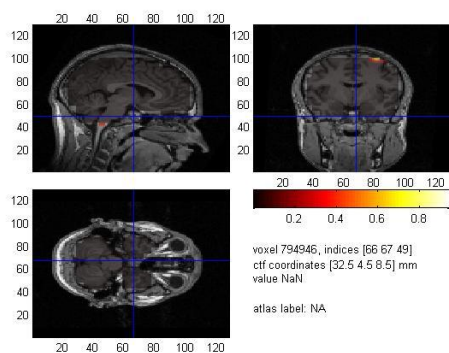


Simulation results

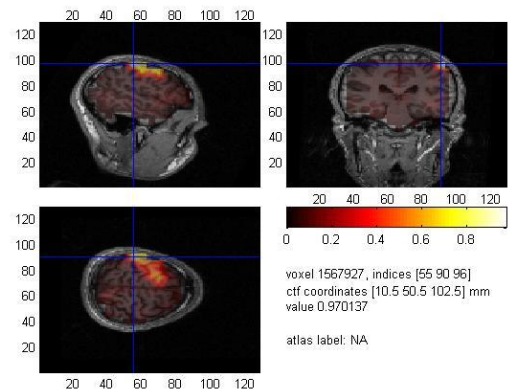


Scenario 6

Test sources

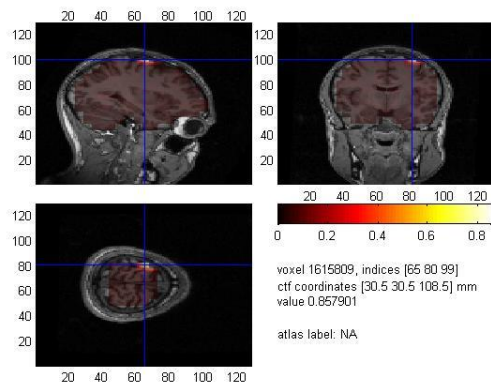


Simulation results

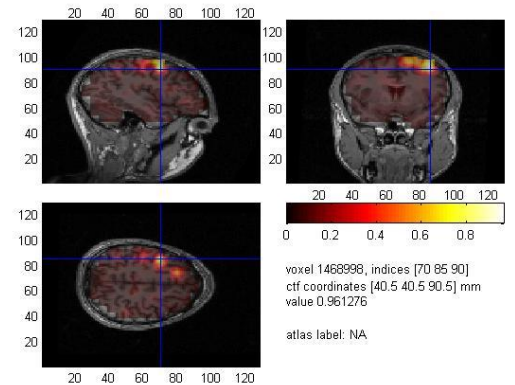


Scenario 7

Test sources

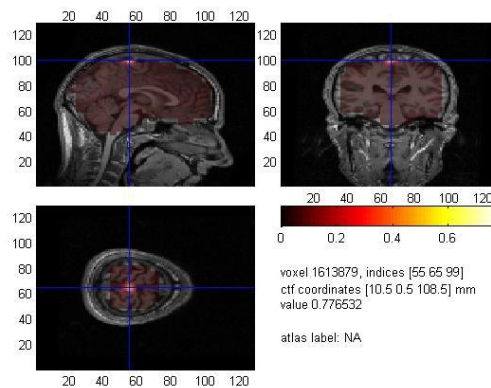


Simulation results

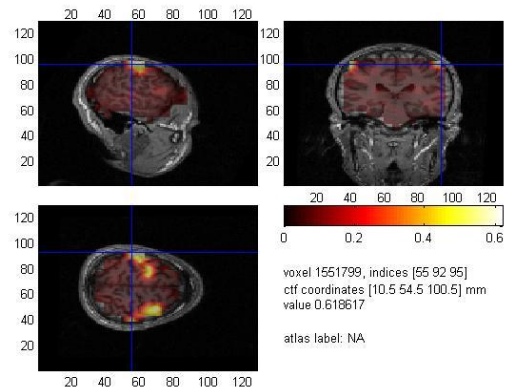


Scenario 8

Test sources

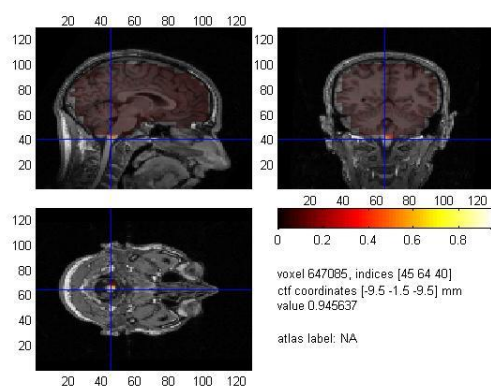


Simulation results

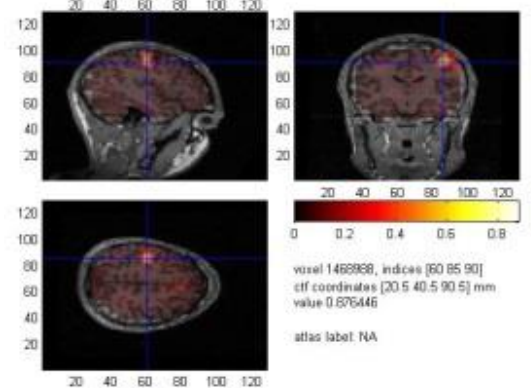


Scenario 9

Test sources

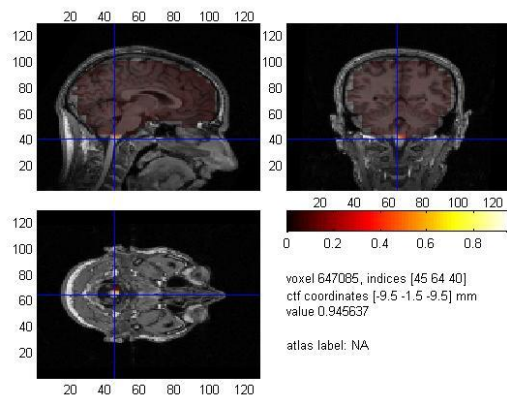


Simulation results

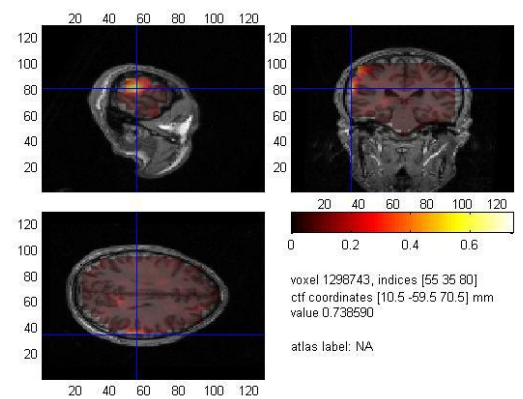


Scenario 10

Test sources

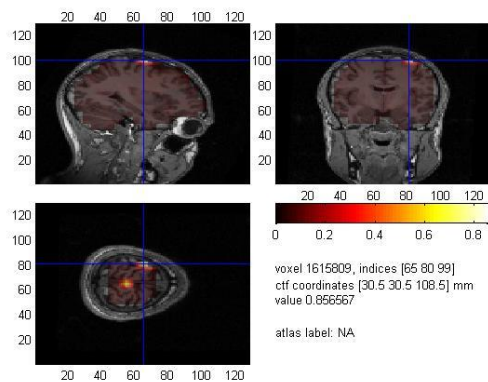


Simulation results

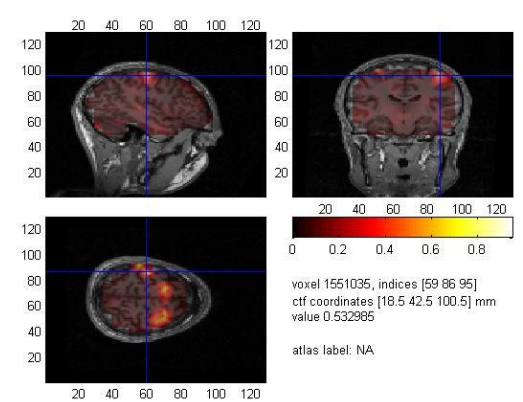


Scenario 11

Test sources

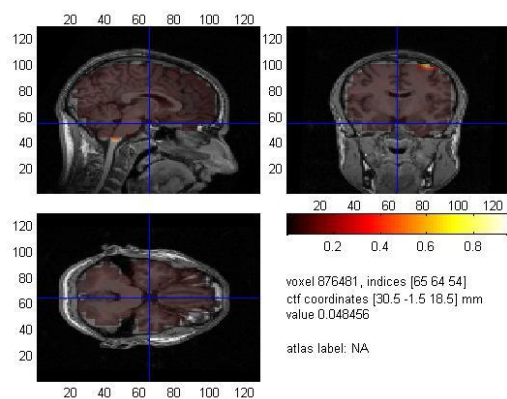


Simulation results

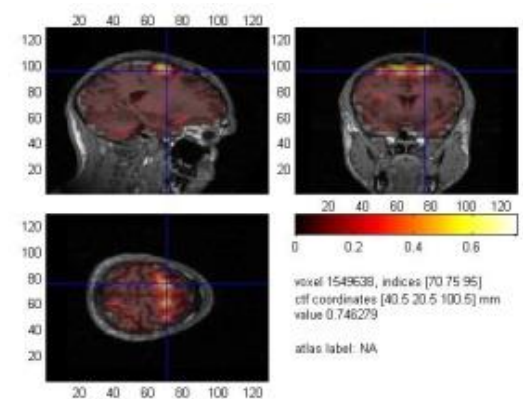


Scenario 12

Test sources



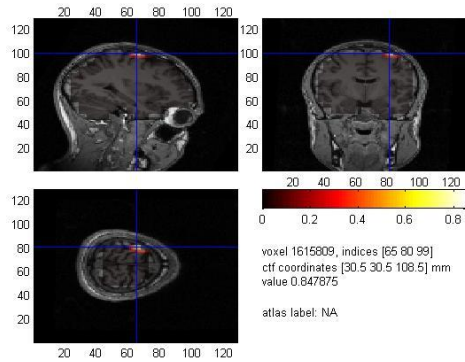
Simulation results



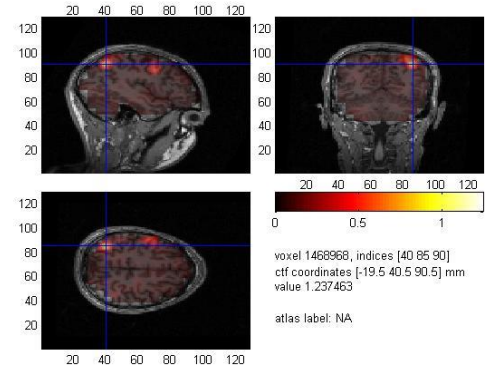
METHOD IV

Scenario 1

Test sources

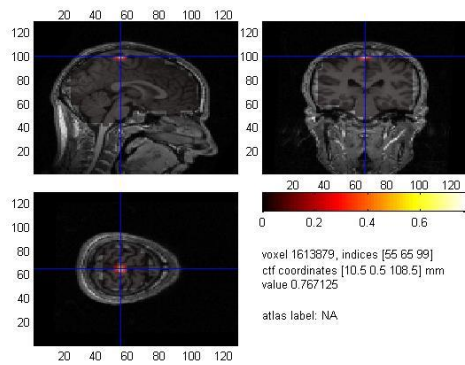


Simulation results

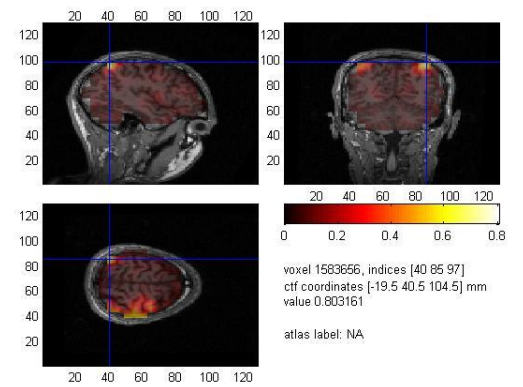


Scenario 2

Test sources

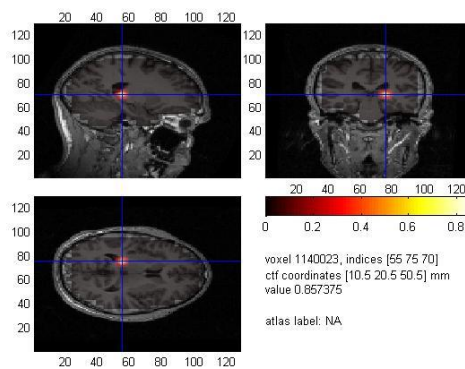


Simulation results

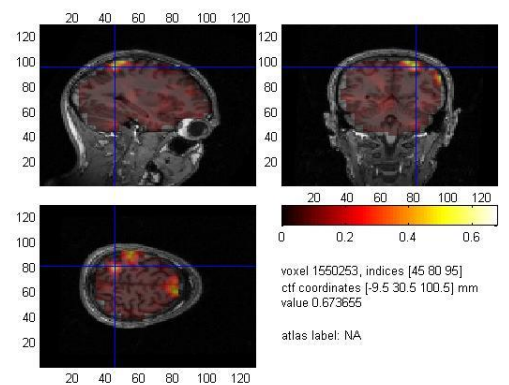


Scenario 3

Test sources

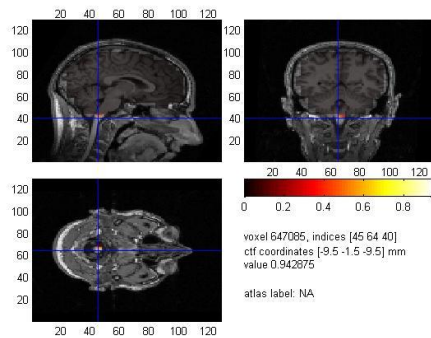


Simulation results

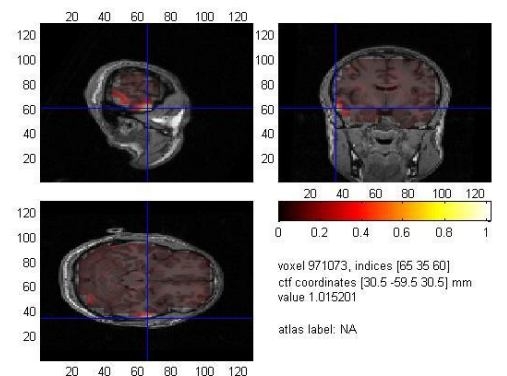


Scenario 4

Test sources

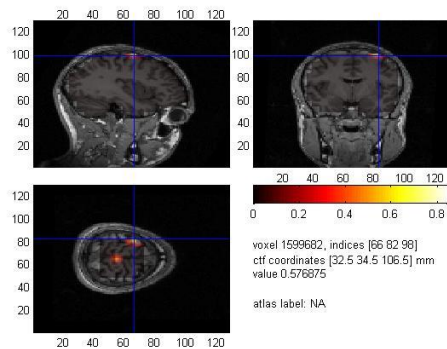


Simulation results

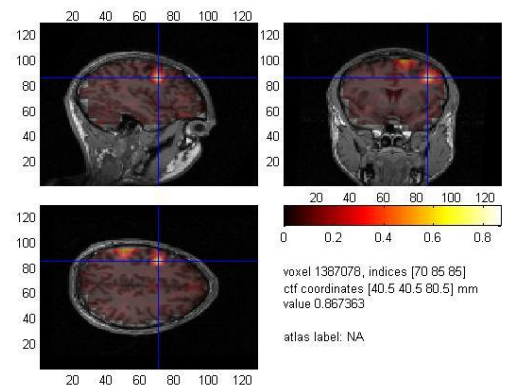


Scenario 5

Test sources

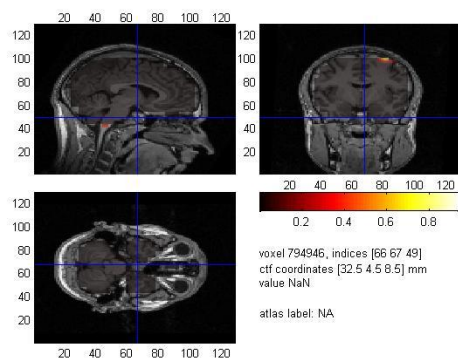


Simulation results

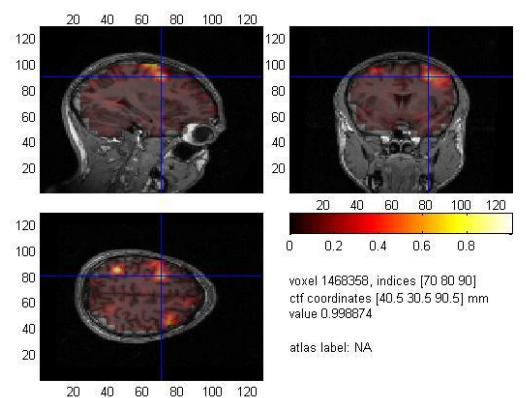


Scenario 6

Test sources

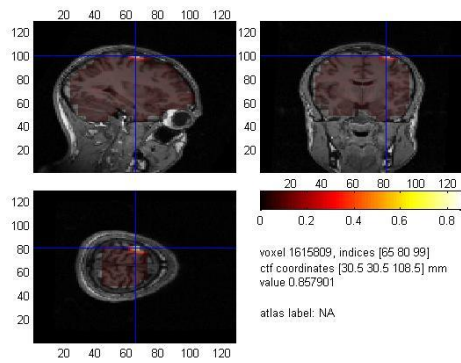


Simulation results

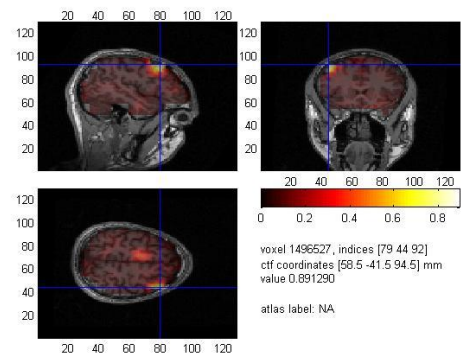


Scenario 7

Test sources

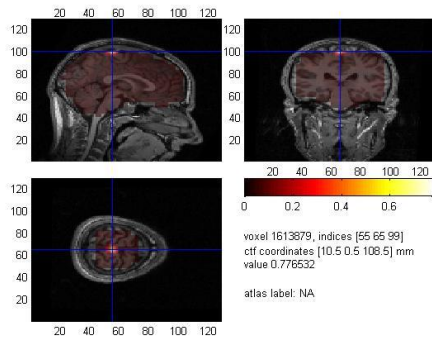


Simulation results

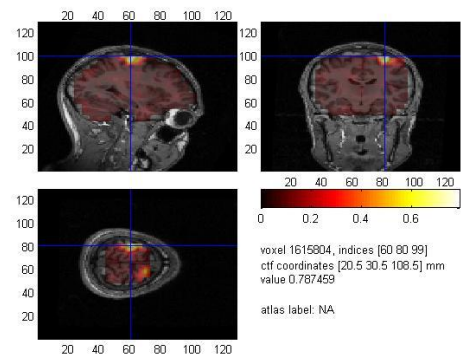


Scenario 8

Test sources

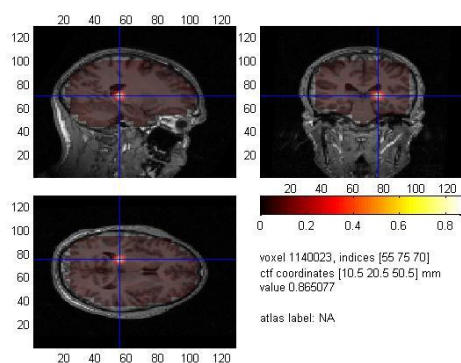


Simulation results

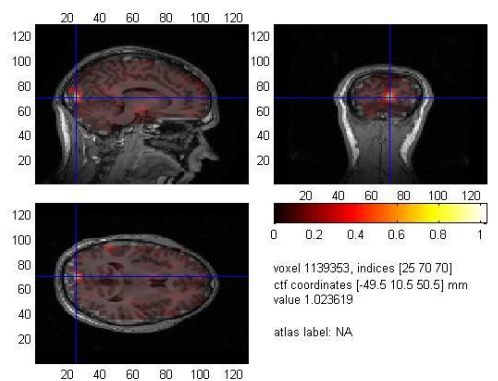


Scenario 9

Test sources

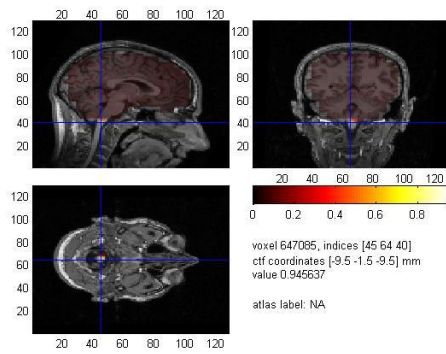


Simulation results

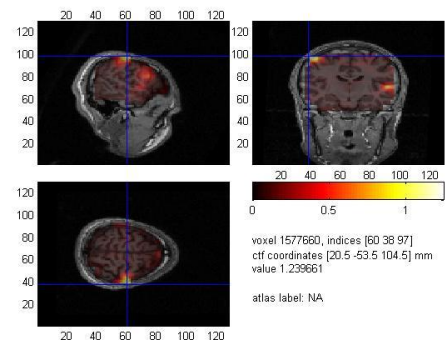


Scenario 10

Test sources

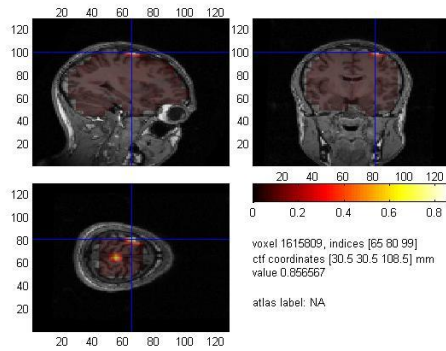


Simulation results

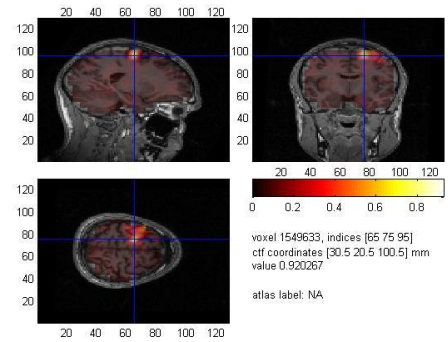


Scenario 11

Test sources

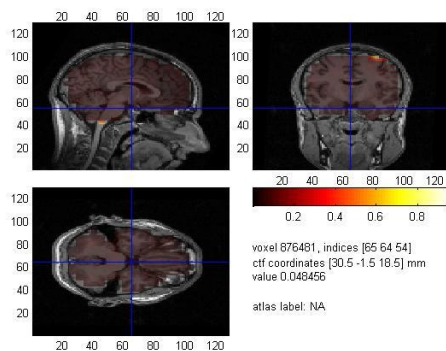


Simulation results

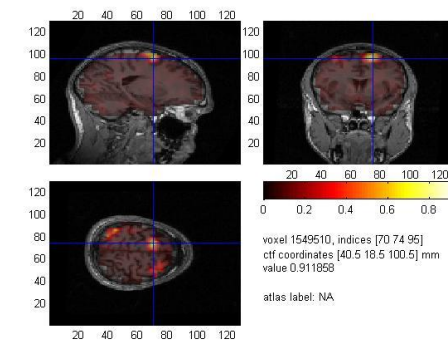


Scenario 12

Test sources



Simulation results



Performance Analysis

- **Quantitative study**

In this section it will be compared the performance of each of the variations of the method applied to each of the twelve different scenarios by computing their quality factor Q . The results are shown in Fig (7).

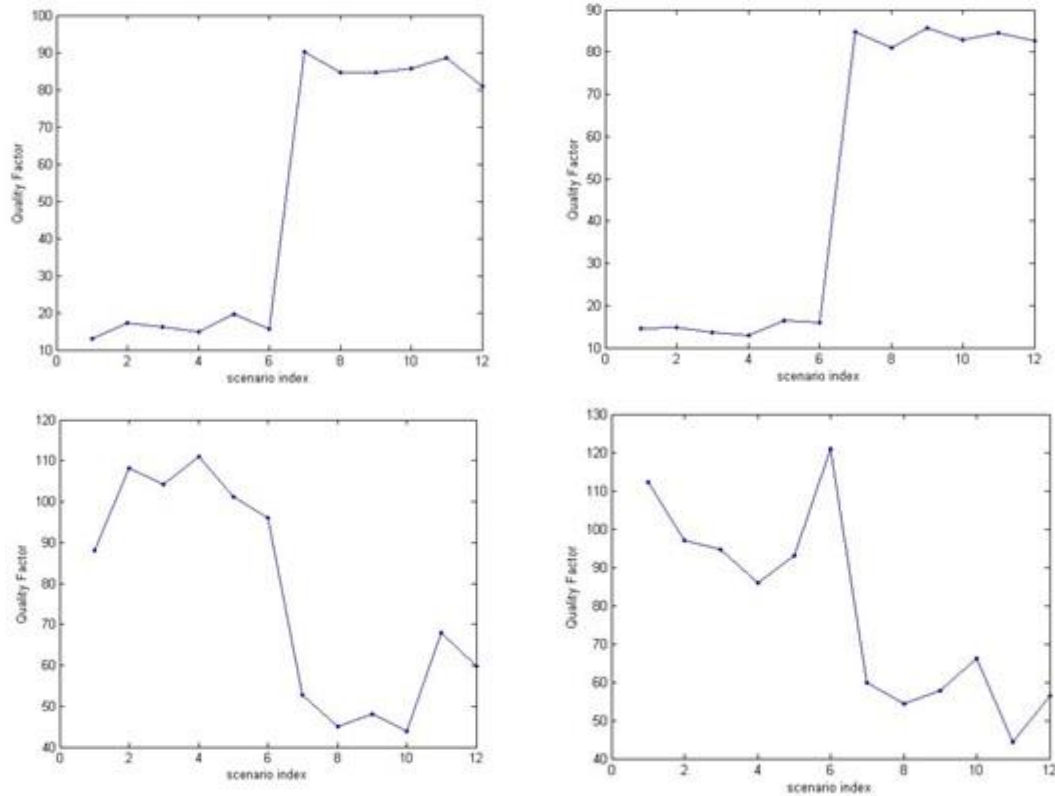


Fig 7. Quality factor of each of the four solving method applied to each of the twelve scenarios.

By simple inspection of the results shown in Fig 7 it can be realized the huge difference between the *noisy* and *concentrated* solving methods. The concentrated methods perform reasonably well in the first six scenarios, which are the ones without any noise.

For the *noisy* strategies the performance increases for the last six scenarios, but the overall performance is, in general, worse than for the previous strategies.

- **Qualitative study**

The ability of the methods to locate correctly the test sources can also be estimated by simple inspection of the anatomical images shown in the previous chapter.

The first method works reasonably well for the first two scenarios. Although the source is reconstructed more diffused than the original, the method is able to locate the activated area. This is not the case for scenarios three and four. In those cases, where deep sources are involved, the method fails dramatically, because it estimates the superficial sources instead of deep ones. The method succeeded again for the scenario 5 (two independent superficial

sources). In this case the spatial estimation is not very accurate but the method is able to differentiate two activated regions. For the scenario 6, the method fails again because it is not able to locate a deep source. The performance is quite similar for the *noisy* scenarios. Although the factor Q increases, due to the addition of many terms in Eq (9), the method performance is not really affected compared to the scenarios 1-6.

The second method performs quite similar to the first one. There is however an exception in the first scenario where the method performs worse than the first one.

The third method is the *noisy* version of the first one. According to the anatomical images it seems that this noisy version leads to worse results than the *concentrated* one. This version is still unable to work out correctly the scenarios with deep sources. Furthermore, it generates less quality estimations of the scenarios one and two, which were correctly estimated by method 1.

The last method is the *noisy* version of the second one. It again, performs worse than its *concentrated* version, method two. Actually, comparing the results of methods three and four it can be realized that the fourth method is the one that leads to the worst results.

4. Discussion

The first important thing to realize is that the performance of all the solving methods depends dramatically in the type of scenario considered. The scenarios with only superficial sources are solved accurately but all methods fail systematically in the scenarios with deep sources. This feature is related with the nature of the inverse problem. The superficial sources are closer to the sensor space than the deep ones, so their gain is localized in a few sensors, which are the closest sensors to the source position. On the other hand, the gain spectrum of a deep source is very flat. This means that almost all the sensors are affected in the same way by a deep source, making it very difficult to extract any information from the sensor data. None of the methods is able to estimate the deep sources, because one of the assumptions is to look for the *easiest solutions*. These easiest are more likely to be superficial sources than deep ones. This is an important challenge to be overcome because some of the most interesting brain research involves deep areas of the brain. This is the case of the research on the Alzheimer disease.

Secondly, all the work was carried out using only one temporal measurement. This automatically excludes the use of any statistical technique that could help to improve the method. However a MEG data set is usually composed by several *trials* or repetitions of the same experiment. Thus, it might be helpful to complement a heuristic method with some information from any statistical parameter extracted from the trials. It could be done making use of the covariance matrix of the data.

Finally this work shows the risk of using a priori assumptions in MEG localizing methods. Although it is necessary to constrain a *minimum-norm* search in order to avoid *overfitting* an abuse of assumption can exclude the correct solution. It is the case of the *easiest solution* assumption which automatically discards the activation of deep sources. Instead it would be very useful to use *tailored assumptions* for each patient or experiment. Those assumptions could arise from a patient clinical data. As it would be the case of a disease or malfunction in some specific brain area. But the assumptions could as well arise from the nature of the experiment. It could be the case if the patient is measured while is told to do some task that is known that involves some specific region of the brain.

Summarizing, this work demonstrated the potential of a guided heuristic method to solve some specific MEG problems. The method is not definitive because do not work correctly for a general MEG scenario. However, the epistasis of the MEG inverse problem suggest that it might be successfully faced using a heuristic method. Consequently, after some improvements, a heuristic based approach may help to clarify the controversial issue of the MEG inverse problem.

5. References

- [1] Hämäläinen M., Hari R., Ilmoniemi R. J., Knuutila J., Lounasmaa O.V. (1993) "Magnetoencephalography - theory, instrumentation, and applicationsto noninvasive studies of the working human brain". *Reviews of Modern Physics*, Vol 65, No. 2, April 1993.
- [2] *Functional MR Imaging (fMRI) - Brain*, American College of Radiology & Radiological Society of North America, May 24, 2011
- [3] Katrina Wendel et al. "EEG/MEG Source Imaging: Methods, Challenges and Open issues". Hindawi publishing. Computational intelligence and Neuroscience. Volume 2009, Article ID 656092.
- [4] Gerard J. Tortora and Bryan H. Derrickson, "Principles of Anatomy and Physiology, 13th Edition. John Wiley & Sons, Inc.
- [5] "Sincronización y coherencia en la actividad cerebral". Alfonso de Hoyos y Fernández de Córdova. PhD Thesis.
- [6] D. Drung, C. Assmann, J. Beyer, A. Kirste, M. Peters, F. Ruede, and Th. Schurig (2007). "Highly sensitive and easy-to-use SQUID sensors". *IEEE Transactions on Applied Superconductivity* **17** (2): 699.
- [7] Press, WH; Teukolsky, SA; Vetterling, WT; Flannery, BP (2007). "Section 19.4. Inverse Problems and the Use of A Priori Information". *Numerical Recipes: The Art of Scientific Computing* (3rd ed.). New York: Cambridge University Press.
- [8] Genetic algorithm. Review and application. Manoj Kumar, Mohammad Husian, Naveen Upreti & Deepti Gupta. International Journal of Information Technology and Knowledge Management. July-December 2010, Volume 2, No. 2, pp. 451-454
- [9] Kirkpatrick, S.; Gelatt, C. D.; Vecchi, M. P. (1983). "Optimization by Simulated Annealing". *Science* **220** (4598): 671–680.
- [10] Storn, R.; Price, K. (1997). "Differential evolution - a simple and efficient heuristic for global optimization over continuous spaces". *Journal of Global Optimization* **11**: 341–359.
- [11] Robert Oostenveld, Pascal Fries, Eris maris and Jan-Mathijs Schoffelen. "Fieldtrip: Open Source Software for Advanced Analysis of MEG EEG, and Invasive electrophysiological Data". Hindawi Publishing Corporation. Computational intelligence and Neuroscience. Volume 2011, Article ID 156869.

